Electronic Supplementary Information

Passive sampling of herbicides combined with effect analysis in algae using a novel high-throughput phytotoxicity assay (Maxi-Imaging-PAM)

[5] **Beate I. Escher,*[a] Pam Quayle[b], Renee Muller[b], Ulrich Schreiber[c], and Jochen F. Mueller[b]**

Chlorophyll fluorescence bioassay

The newly developed Maxi-Imaging-PAM chlorophyll fluorometer (IPAM) (first prototype manufactured by J. Kolbowski and U.Schreiber, Würzburg, Germany; series production by Heinz Walz GmbH, Effeltrich, Germany) essentially is based on the same measurement principle as the ToxY-Pam used in our earlier studies [1-5]. For the purpose of the present study it is advantageous that the new system is based on chlorophyll fluorescence imaging of a large sample area (10x13 cm) offering the opportunity to simultaneously assess the fluorescence properties and, hence, photosynthetic activity of a large number of samples, e.g. in 96-well plates. Details on the instrument and methodology are described in [6,7]. Briefly, 200 to 350 µl of algal suspension of *Chlorella vulgaris* grown as described in [6,7], were pipetted in each well. For each plate a fixed amount of algae was used and the final volume of each well was 370 µl. Algae were exposed to blue (460 nm) actinic illumination with a quantum flux density of photosynthetically active radiation (PAR) of 7 μmol_{quanta} m^{-2} s^{-1} during the entire incubation time. After an incubation of 20 min in the IPAM, a measurement cycle was started.

A measurement with the IPAM involves the application of a saturation pulse which leads to full inhibition of energy conversion at PS II reaction centers and, hence, transiently induces maximal fluorescence yield (see [8] for a recent review on PAM fluorometry and the saturation pulse method). One measurement cycle consisted of 10 saturation pulses 1 min apart from each other during each of which the maximum fluorescence yield F_M' was measured. Briefly before each saturation pulse the momentary fluorescence yield, F, was assessed. The effective quantum yield of energy conversion at photosystem II reaction centers, Y, was computed using eq. 6 and the yield values Y of the last 5 measurements of a cycle were averaged.

$$Y = \left(\frac{F_M' - F}{F_M'} \right) \tag{1}$$

Then varying concentrations/volumes of reference compounds or extracts diluted with water were added to each well making up a total volume of 370 µl and the plate was again incubated at a PAR of 7. After 1, 2, 3, 4, 5, 6, 22, 23 and 24 h a measurement cycle was performed. The inhibition of photosystem II quantum yield was calculated using eq. 7.

$$\text{inhibition } [\%] = \left(1 - \frac{Y_{sample}}{Y_{control}} \right) \cdot 100\% \tag{2}$$

As the effective quantum yield, Y, decreases with increasing PAR, correct determination of inhibition requires homogenous illumination of sample and control wells. Illumination of the individual wells by the LED-array of the IPAM displayed a maximal deviation of +/- 10% from the mean PAR of all 96 wells with positive and negative deviations being unevenly distributed over the multiwell plate. For evaluation of the resulting error, it has to be considered that at 7 µmol quanta m^{-2}s^{-1} a +/-10% variation of PAR results in maximal deviation of only 1% of inhibition (%) from the mean value [7]. Although the resulting error may be ignored in most practical applications, the plate was divided in 8 quadrants. The left 4 wells of each quadrant were controls, three of which were filled with water and one with the positive control diuron. The average of the Y-values of the water wells in the adjacent quadrant at each given time point are the $Y_{control}$ in eq. 7.

Concentration-Effect Curves of the Reference compounds

The concentration-effect curves of diuron and simazine measured with the IPAM were independent of exposure time from 1 to 25 hours under the incubation conditions chosen in this study (Figures 1A and 2). Diuron followed a log-logistic curve with a slope $s_D = 1.00\pm0.08$ (Figure 1A). The response pattern was typical for an PSII inhibitor. The maximum fluorescence stayed virtually constant (Figure 1C), while F increased (resulting in a negative inhibition of F) (Figure 1B). This response pattern is caused by the closing of the acceptor site followed by a total block of the

[a] *Department of Environmental Toxicology, Swiss Federal Institute for Aquatic Science and Technology (Eawag), CH-8600 Dübendorf, Switzerland. Fax: 0041 44 823 5471; Tel: 0041 44 823 5068; E-mail: escher@eawag.ch*
[b] *The National Research Centre for Environmental Toxicology (EnTox), The University of Queensland, Brisbane, QLD 4072, Australia. E-mail: j.muller@uq.edu.au*
[c] *Julius-von-Sachs Institut für Biowissenschaften, Lehrstuhl Botanik I, University of Würzburg, D-97082 Würzburg, Germany, Würzburg, Germany, Fax: 49-931-784-2110; Tel: 49-931-784-2110; E-mail: ulrichschreiber@gmx.de*

$$\text{inhibition } [\%] = \left(1 - \frac{Y_{sample}}{Y_{control}}\right) \cdot 100\% \qquad \text{inhibition } [\%] = \left(1 - \frac{F_{sample}}{F_{control}}\right) \cdot 100\% \qquad \text{inhibition } [\%] = \left(1 - \frac{F'_{M\ sample}}{F'_{M\ control}}\right) \cdot 100\%$$
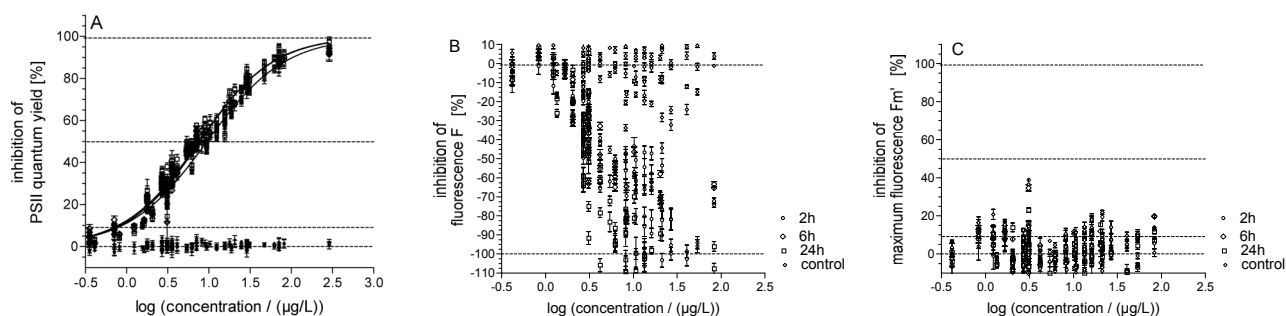

Fig. 1 Concentration-effect curves of diuron. A. Photosynthesis yield Y, B. Fluorescence F, C. Maximum fluorescence Fm'. For better visibility, only the data points from the following exposure times are plotted: ◆ control 0h ○ 2h, ◇ 6h, □ 24h.

electron transfer. Thus all energy is directly converted to fluorescence.

Simazine neither reached the 100% level nor was the slope equal to 1 (Figure 2). In order to implement relative potencies, and for the EC_{10} to be derived from an absolute, not a relative 10% effect level, the curve fit for simazine was forced to be parallel to the diuron curve, i.e., slope was fixed to 1.00 and the top of the curve was fixed at 100% effect level (Table 3 of the main manuscript). Note however, that the resulting EC_{10} did not differ much from that derived with a fitted top and slope (s = 0.91 ±0.04), resulting in an EC_{10} of 5.26 µg/L (95% confidence interval: 4.68 to 5.91).

While toxicity of the PSII inhibitors was independent of time under the low light conditions chosen here (7 µE m^{-2}s^{-1}), the toxicity of phenol almost doubled within 24 h (Figure 3). In addition, the concentration-effect curve of phenol with a slope of 4.54±0.81 was much steeper than that of diuron (s_D = 1.00±0.09). Also, the inhibition of Y surpassed the 100% level. This obervation can be understood if the response pattern is analyzed. Both F and Fm' are inhibited (Figures 3B and 3C) partially due to nonspecfic toxicity which leads to killing of the cells. In addition, there is an effect on the photosynthesis yield but only at higher concentrations. Thus apparently the inhibition of photosynthesis is only a secondary effect.

These differences between the baseline toxicant phenol and the PSII inhibitors are consistent with the mode of toxic action of the different reference compounds. The action of diuron and simazine should set in relatively fast after addition because they act by binding to the PSII and the effect is limited by toxicokinetics (bioconcentration and partitioning to binding site), while the baseline toxicant phenol does not act directly or specifically on PSII. Thus a slower response time can be expected. In fact for such mechanisms, effects on growth and reproduction of algae sets in at lower concentrations and shorter incubation times than effects on PSII quantum yield (M. Koller, Eawag, unpublished data). Therefore direct inhibition of photosynthesis is only a secondary and less sensitive effect.

Given the high sensitivity of the assay to PSII inhibitors and the low effect of non-specifically acting compounds even at rather high concentrations, one can conclude that the assay is rather selective for PSII inhibitors and should not be too much disturbed by the matrix components in POS extracts.
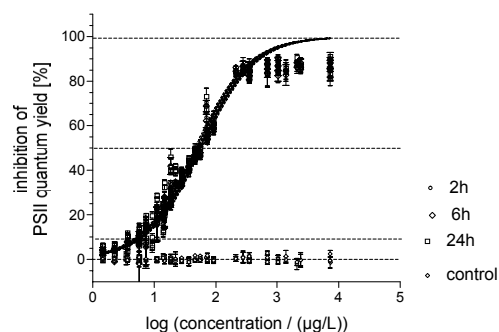

Fig. 2 Concentration-effect curves of simazine. ◆ control 0h, ○ 2h, ◇ 6h, □ 24h.

References

1   U. Schreiber, J. Müller, A. Haugg and R. Gademann, *Photosynth. Res.*, 2003, **74**, 317-330.

2   S. M. Bengtson Nash, K. Mcmahon, G. Eaglesham and J. F. Muller, *Marine Pollution Bulletin*, 2005, **51**, 351-360.

3   S. M. Bengtson Nash, U. Schreiber, P. J. Ralph and J. F. Muller, *Biosensors and Bioelectronics*, 2005, **20**, 1443-1451.

4   B. I. Escher, N. Bramaz, R. I. L. Eggen and M. Richter, *Environ. Sci. Technol.*, 2005, **39**, 3090-3100.

5   B. I. Escher, N. Bramaz, M. Maurer, M. Richter, D. Sutter, C. Von Känel and M. Zschokke, *Environ. Tox. Chem.*, 2005, **24**, 750-758.

6   S. Schmidt Development and evaluation of the Maxi-Imaging-PAM algae assay using 96 well plates, National Research Centre for Environmental Toxicology (EnTox), 2005.

7   U. Schreiber, P. Quayle, S. Schmidt, B. I. Escher and J. Mueller, *Biosensors and Bioelectronics*, 2006, submitted.

8   U. Schreiber, In *Chlorophyll Fluorescence: A Signature of Photosynthesis*; G. Papageorgiou, Govindjee, Eds.; Kluwer Academic Publishers: Dordrecht, The Netherlands, pp 279-319, 2004.
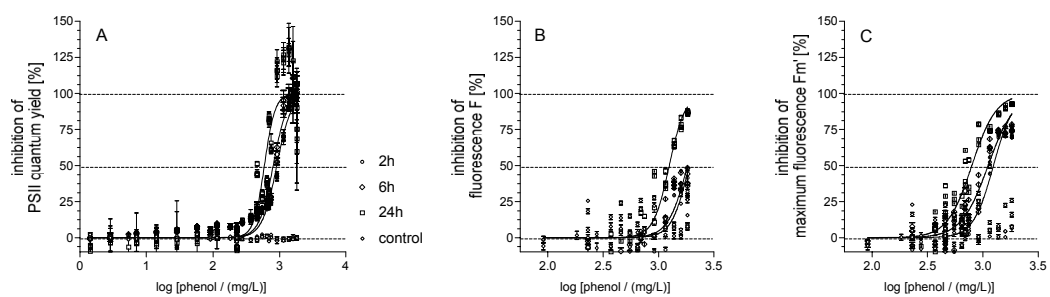
Fig. 3 Concentration-effect curves of phenol. A. Photosynthesis yield Y, B. Fluorescence F, C. Maximum fluorescence Fm'. For better visibility, only the data points from the following exposure times are plotted: ◆ control 0h ○ 2h, ◇ 6h, □ 24h.